2013 IEEE/RSJ International Conference on
Intelligent Robots and Systems (IROS)
November 3-7, 2013. Tokyo, Japan

A Modular Aerial Vehicle with Redundant Actuation

Roberto Naldi, Alessio Riccò, Andrea Serrani, Lorenzo Marconi

Abstract— **This work presents the design and experimental validation of a control strategy for an innovative modular aerial vehicle characterized by redundant actuation. For this class of aircraft, the distinguishing feature of the proposed design – which sets it apart from standard vertical take-off and landing (VTOL) under-actuated configurations such as helicopters, ducted-fan tail-sitters or multi-rotors – is that the input redundancy can be employed to improve the dynamical properties of the system. In particular, the vehicle performance can be enhanced in certain applications that benefit from a larger number of degrees of freedom being simultaneously controlled. A control strategy is proposed which is capable of globally stabilizing the dynamics of this class of vehicles along a desired trajectory. The methodology is validated by means of experiments carried out on a special prototype obtained by rigidly connecting two ducted-fan tail-sitter UAVs.**

I. Introduction

Miniature under-actuated VTOL aerial vehicles are successfully employed in a large variety of applications including, among others, surveillance, aerial photography and search and rescue operations [1]. One reason for this widespread success is the high level of dexterity and maneuverability that allow these vehicles to operate in real world mission scenarios and populated environments. Among the most successful vehicle configurations of this kind are helicopters - [2], [3] - ducted-fan tail-sitters - [4], [5] - and multi-propeller systems - [6], [7], [8], [9]. Despite a significant variability in aero-mechanical design, all the aforementioned aerial systems share a similar dynamical behavior that reflects the under-actuated nature of their dynamics. More specifically, by considering the so-called vectored-thrust approximation [10], these vehicles are often considered as rigid bodies driven by four independent control inputs given by the main thrust and three control torques along the principal axes of inertia. As a consequence, not all their six degrees of freedom can be controlled simultaneously; rather, the vehicle attitude must be manipulated to control the vehicle translational motion. This fact may limit the control effectiveness of the system during certain operations that require a high level of dexterity and accuracy. To overcome these limitations, for some specific application scenarios several innovative configurations have been proposed where this issue has been mitigated by a suitable mechanical design. For example, in [11], [12] and [13], aerial systems endowed with robotics arms have been considered. Additional degrees of freedom are obtained by jointly controlling the arm and the aerial vehicle so as to accomplish advanced robotics operations, including manipulation. In [14], an additional propeller is employed to let a quadrotor aerial vehicle apply forces towards a vertical surface while hovering. In [15], a fully actuated behavior is obtained for a quadrotor by the introduction of additional actuators, namely by endowing the propellers with tilting capabilities. In [16] and [17], a new class of modular aerial vehicles has been proposed, which is obtained by rigidly connecting a number of under-actuated modules based on a standard ducted-fan configuration. For these modular systems, the number of independently controlled degrees of freedom of the overall assembly can be larger than the one of the single units, depending on the number of modules and the topology of their interconnection. This makes it possible to achieve full 6-DOF actuation in certain configurations.

As a natural development from the preliminary results obtained in [16] and [17], this work presents the design and the experimental validation of a control strategy for a particular aerial vehicle obtained by rigidly connecting two ducted-fan modules. The resulting system, which has been specifically designed to accomplish operations requiring physical interaction with the environment, is characterized by an additional control direction compared to the standard vectored-thrust under-actuated dynamical model of the single unit. By taking advantage of this redundancy in the input space, the proposed control law is capable to globally stabilize a desired trajectory that would not be feasible for a single unit, but becomes attainable for the modular system due to its enhanced dynamic behavior. The effectiveness of the proposed control strategy is demonstrated by means of experiments considering both free-flight maneuvers as well as a physical interaction with the environment.

A. Notation and Definitions

Throughout this paper, $\mathcal{F}_i$ and $\mathcal{F}_b$ denote, respectively, an inertial reference frame and a reference frame attached to the center of gravity of the vehicle. With $I_n \in \mathbb{R}^{n\times n}$ we denote the n-dimensional identity matrix. With e_1, e_2 and e_3 we denote the unit vectors $e_1 := [1, 0, 0]^T$, $e_2 := [0, 1, 0]^T$ and $e_3 := [0, 0, 1]^T$. For any $x \in \mathbb{R}^3$, we let

$$S(x) := \begin{bmatrix} 0 & -x_3 & x_2 \\ x_3 & 0 & -x_1 \\ -x_2 & x_1 & 0 \end{bmatrix}$$

This research has been conducted under the collaborative project SHERPA (Smart collaboration between Humans and ground-aErial Robots for imProving rescuing activities in Alpine environments) supported by the European Community under the 7th Framework Programme.

R. Naldi, A. Riccò and L. Marconi are with CASY-DEI, Università di Bologna, Bologna, 40133, Italy, roberto.naldi@unibo.it, alessio.ricco@studio.unibo.it, lmarconi@unibo.it.
A. Serrani is with the Department of Electrical and Computer Engineering, The Ohio State University, Columbus, OH 43210 - USA, serrani@ece.osu.edu. Corresponding author: Roberto Naldi, roberto.naldi@unibo.it.

be a skew-symmetric matrix and we denote with $^\wedge$ the inverse operator such that $S(x)^\wedge = x$. With S_n we denote the n-dimensional unit sphere defined as $S_n := \{x \in \mathbb{R}^{n+1} : \|x\| = 1\}$. With $B_n(r)$ we denote the n-dimensional ball of radius r, namely $B_n(r) := \{x \in \mathbb{R}^n : \|x\| \leq r\}$. A unit quaternion $q \in S_3$ is defined as a pair $q = [\eta, \epsilon^T]^T$ where $\eta \in \mathbb{R}$ and $\epsilon \in \mathbb{R}^3$ are denoted respectively the scalar and the vector part. Given unit quaternions $q_1 = [\eta_1, \epsilon_1^T]^T$ and $q_2 = [\eta_2, \epsilon_2^T]^T$, the standard quaternion product is defined as

$$q_1 \otimes q_2 = \begin{bmatrix} \eta_1 & -\epsilon_1^T \\ \epsilon_1 & \eta_1 I_3 + S(\epsilon_1) \end{bmatrix} \begin{bmatrix} \eta_2 \\ \epsilon_2 \end{bmatrix}.$$

For a quaternion $q = [\eta, \epsilon^T]^T \in S_3$, we have $q \otimes q^{-1} = q^{-1} \otimes q = \mathbf{1}$ with $q^{-1} = [\eta, -\epsilon^T]^T$ being the inverse and $\mathbf{1} = [1, 0, 0, 0]^T \in S_3$ the identity quaternion element. Given a set S, $\text{coni}(S)$ denotes the conic hull of S.

We refer to a *saturation function* as a mapping $\sigma : \mathbb{R}^n \to \mathbb{R}^n$ such that, for $n = 1$,

1) $|\sigma'(s)| := |d\sigma(s)/ds| \leq 2$ for all s,
2) $s\sigma(s) > 0$ for all $s \neq 0$, $\sigma(0) = 0$,
3) $\sigma(s) = \text{sgn}(s)$ for $|s| \geq 1$,
4) $|s| < |\sigma(s)| < 1$ for $|s| < 1$.

For $n > 1$, the properties listed above are intended to hold componentwise.

II. Dynamical Model

The aerial vehicle considered in this work consists of a modular ducted-fan configuration [16] obtained by combining two separate ducted-fan UAVs. Each ducted-fan module [5] can be thought as comprised by two main subsystems. The first one is given by a fixed-pitch propeller driven by an electric motor. This subsystem is responsible for generating the main thrust required to counteract the gravity force. The second subsystem is given by a set of actuated control surfaces acting on the airflow generated by the propeller. This subsystem is able to produce a certain number of aerodynamic moments so as to govern the attitude dynamics of each single module. In summary, following the analysis in [5], each module can be regarded as a rigid body driven by four control inputs, namely a force input corresponding to the propeller's thrust and three torque inputs obtained by means of the actuated control surfaces. The idea behind the proposed modular configuration is to obtain, by suitably combining the effects of the actuators on each different module, an additional control force. The following subsections present the dynamical model of this class of systems and a comparison with the standard vectored-thrust under-actuated dynamics which characterize a single module.

A. Vectored Thrust Dynamical Model (VT4)

A large class of under-actuated (VTOL) aerial systems, including quadrotors, helicopters and (single module) ducted-fans configurations, is typically modeled by the so called vectored-thrust dynamical model [18]

$$\begin{aligned} M\ddot{p} &= -u_f R e_3 + M g e_3 \\ \dot{R} &= RS(w) \\ J\dot{w} &= S(Jw)w + u_\tau \end{aligned} \tag{1}$$

where $p = [x, y, z]^T \in \mathbb{R}^3$ denotes the position of the center of gravity of the system expressed in the inertial reference frame $\mathcal{F}_i$, $w = [w_x, w_y, w_z]^T \in \mathbb{R}^3$ is the angular velocity expressed in the body frame $\mathcal{F}_b$, $R \in SO(3)$ is the rotation matrix relating vectors in $\mathcal{F}_b$ to vectors in $\mathcal{F}_i$, $M > 0$ and $J \in \mathbb{R}^{3\times 3}$ (with the property that $J = J^T > 0$) denote respectively the mass and the inertia matrix of the vehicle, $u_f \in \mathbb{R}_{\geq 0}$ is the control force generated by the aircraft own actuators (which, by construction, is directed along the body z axis) and, finally, $u_\tau \in \mathbb{R}^3$ is the vector of control torques.

The distinguishing feature of the vectored-thrust dynamical model (1) is the fact that the translational dynamics can be controlled by tilting the vehicle with respect to the inertial frame (i.e., by changing the orientation R through the torque control input) and by controlling the magnitude of a single force vector modeling the resultant force produced by the onboard propellers. Since the dynamics in (1) are characterized by four different control inputs (the thrust magnitude u_f and the three torques u_τ), we will compactly denote the model as (VT4).

To take saturation of the actuators into account, the following constraints on the admissible values of the control inputs are introduced

$$u_f \in \Omega_f, \quad u_\tau \in \Omega_\tau \tag{2}$$

where the compact sets $\Omega_f \subset \mathbb{R}_{\geq 0}$, $\Omega_\tau \subset \mathbb{R}^3$ specify the attainable control force and torques for the specific vehicle.

B. Vectored bi-directional Thrust Dynamical Model (VT5)

Following [16], the modular system considered in this work is described by a model where, as opposed to (1), two force vectors can be manipulated. Specifically, the model reads as

$$\begin{aligned} M\ddot{p} &= -u_{f_1} R e_3 + u_{f_2} R e_k + M g e_3 \\ \dot{R} &= RS(w) \\ J\dot{w} &= S(Jw)w + u_\tau \end{aligned} \tag{3}$$

where $k \in \{1, 2\}$ and $u_{f_1} \in \mathbb{R}_{\geq 0}$, $u_{f_2} \in \mathbb{R}$ denote the two control forces which can be generated by the aircraft own actuators. The main property of the above mathematical model is that the second additional force vector of magnitude u_{f_2} is perpendicular to the one of magnitude u_{f_1} (see Figure 1). Accordingly, the dynamics in (3) are characterized by five different control inputs: the magnitudes of the two control forces u_{f_1}, u_{f_2} and the three-dimensional torque u_τ. Due to this particular structure, this model will be compactly denoted as (VT5). Finally, to take into account actuator saturations, the following constraints are introduced:

$$u_{f_1} \in \Omega_f, \quad u_{f_2} \in \Omega_{f_2}, \quad u_\tau \in \Omega_\tau \tag{4}$$

In addition to (2), the compact set $\Omega_{f_2} \subset \mathbb{R}$ represents the attainable values of the additional control input u_{f_2}.

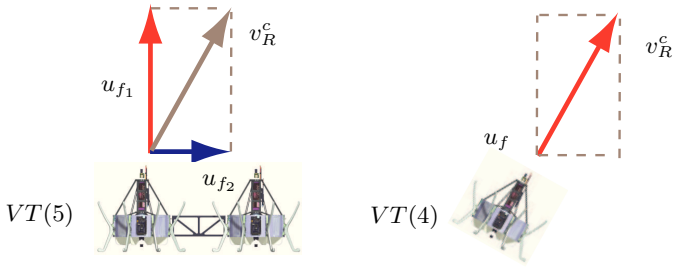

Fig. 1. To generate a desired force control vector, the (VT5) control can take advantage of the additional input u_{f_2} to reduce the constraint on the attitude of the vehicle.

III. Control Problem

The goal of the controller to be designed for the selected aerial configuration is to track a given time reference position and orientation

$$p_R(t) \in \mathbb{R}^3, \quad R_R(t) \in SO(3) \tag{5}$$

which must be chosen to satisfy the *functional controllability* constraints of the system, which are described in the following two subsections for the (VT4) and (VT5) dynamical models, respectively. In particular, due to the under-actuated nature of both the (VT4) and (VT5) dynamics, the attitude reference is required to satisfy some constraints deriving from the position tracking objective. It is shown how the additional control input for the dynamical model (VT5) leads to an additional degree of freedom in choosing the desired orientation compared to the (VT4) case.

A. (VT4) Model Inversion

Let us consider the position dynamics given by the first equation in (1). In order to track the desired trajectory $p_R(t)$ it is possible to define a *reference control force vector* v_R^c as

$$v_R^c(\ddot{p}_R) := Mge_3 - M\ddot{p}_R \tag{6}$$

and then compute a reference orientation R_R and reference control force input u_{f_R} to obtain

$$u_{f_R} R_R e_3 = v_R^c(\ddot{p}_R)\,. \tag{7}$$

The reference attitude $R_R \in SO(3)$ must satisfy

$$R_R e_3 = \frac{v_R^c(\ddot{p}_R)}{\|v_R^c(\ddot{p}_R)\|} \tag{8}$$

meaning that the body z-axis of the vehicle should be aligned with the reference control force vector. Note that, to compute a solution to (8), the reference control force vector should be such that

$$\|v_R^c(\ddot{p}_R(t))\| > v^L, \ \ \forall t \geq 0 \tag{9}$$

for some positive v^L. The reference control force required to track asymptotically the desired position is then given by the magnitude of the reference control force vector

$$u_{f_R} \ := \ \|v_R^c(\ddot{p_R})\|\,. \tag{10}$$

Finally, in order to track the desired orientation, the reference torque input can be computed as

$$u_{\tau_R} \ := \ J\dot{w}_R - S(Jw_R)w_R \tag{11}$$

where w_R is obtained by differentiating the desired attitude R_R satisfying the constraint (8). The reference position $p_R(t)$ and the reference orientation R_R must be chosen to let the control force and torques computed in (10) and (11) satisfy the actuator constraints (2). In practice, fulfillment of these constraints requires $p_R(t)$ and $R_R(t)$ to be sufficiently smooth functions of time satisfying appropriate bounds on the magnitude of their first and second derivatives.

B. (VT5) Model Inversion

Differently from to the algorithm outlined in Section III-A, to obtain the reference control vector $v_R^c(\ddot{p}_R)$ for the position dynamics of (3), the reference rotation matrix R_R and the two reference control force inputs $u_{f_{1R}}$, $u_{f_{2R}}$ must satisfy[1]

$$u_{f_{1R}} R_R e_3 - u_{f_{2R}} R_R e_1 = v_R^c(\ddot{p}_R)\,. \tag{12}$$

Specifically, for the attitude reference R_R it is possible to introduce the following constraint

$$e_3^T R_R^T(t) v_R^c(\ddot{p}_R(t)) \geq v_z^L\,, \quad e_2^T R_R^T(t) v_R^c(\ddot{p}_R(t)) = 0 \tag{13}$$

for all $t \geq 0$, with $v_z^L > 0$. Similarly to the case of the (VT4) model inversion, we require that the reference position satisfies (9). Then, the reference force control inputs can be computed as

$$\begin{aligned} u_{f_{1R}} &= -e_3^T R_R^T v_R^c(\ddot{p}_R) \\ u_{f_{2R}} &= e_1^T R_R^T v_R^c(\ddot{p}_R) \end{aligned} \tag{14}$$

while the reference torque inputs can be computed as in (11) with w_R, $\dot{w}_R$ obtained by differentiating the desired attitude $R_R(t)$ subject to the new constraint (13). As for the (VT4) case, the reference position and orientation $p_R(t)$ and $R_R(t)$ should also be chosen to satisfy the functional controllability of the system, namely $u_{f_{1R}}$, $u_{f_{2R}}$, u_{τ_R} should satisfy the actuator constraints (4).

IV. Control Strategy

The goal of this section is to present a control strategy to solve the control problem defined in Section III. The controller is derived by considering the (VT5) configuration given in (3) as a starting point. The (VT4) case can indeed be considered as a special case of (VT5) resulting from the selection $u_{f_2} \equiv 0$.

A. Position Control

Consider the following error coordinates

$$\bar{p} := p - p_R, \qquad \dot{\bar{p}} := \dot{p} - \dot{p}_R$$

so that the position error dynamics in (3) can be rewritten as

$$M\ddot{\bar{p}} = -u_{f_1} Re_3 + u_{f_2} Re_1 + Mge_3 - M\ddot{p}_R\,. \tag{15}$$

[1]In the remainder of the paper, without loss of generality, it is assumed that $k = 1$.

Following the construction proposed in Section III, it is now possible to define the *control force vector* as

$$v^c(\bar{p}, \dot{\bar{p}}, \ddot{p}_R) := v^c_R(\ddot{p}_R) + \kappa(\bar{p}, \dot{\bar{p}}) \tag{16}$$

where $\kappa(\bar{p}, \dot{\bar{p}})$ a static state feedback control selected as the following *nested saturation feedback law*

$$\begin{aligned} \zeta_1 &:= \bar{p} \\ \zeta_2 &:= \dot{\bar{p}} + \lambda_1 \sigma\left(\frac{k_1}{\lambda_1}\zeta_1\right) \\ \kappa(\bar{p}, \dot{\bar{p}}) &:= \lambda_2 \sigma\left(\frac{k_2}{\lambda_2}\zeta_2\right) \end{aligned} \tag{17}$$

and λ_1, λ_2, k_1 and k_2 are positive gains to be tuned.

The approach is to govern the position dynamics of the vehicle by applying the control force vector (16) to the position dynamics. As for the reference control vector in (12), this can be obtained by suitably controlling the orientation R and selecting the magnitude of the force inputs u_{f_1} and u_{f_2}. In particular, we define the *control attitude* R_c as $R_c = R_R R'_c(\bar{p}, \dot{\bar{p}})$, where $R'_c(\bar{p}, \dot{\bar{p}}) \in SO(3)$ is given by

$$R'_c(\bar{p}, \dot{\bar{p}}) = \begin{bmatrix} 1 & 0 & 0 \\ 0 & \cos\phi_c & -\sin\phi_c \\ 0 & \sin\phi_c & \cos\phi_c \end{bmatrix}$$

being $\phi_c = \pi/2 - \arccos\left(e_2^T R_R^T v^c(\bar{p}, \dot{\bar{p}}, \ddot{p}_R)\right)$. The transformation R'_c rotates the body-frame to let the control vector v^c belong to the subspace spanned by the unit vectors e_1 and e_3 in the body frame. Note that, from the definition of control force vector in (16) and from the properties of the reference attitude in (13), it is possible to choose the saturation parameter λ_2 to guarantee that the angle ϕ_c remains small regardless of the magnitude of the position and velocity errors $\bar{p}$, $\dot{\bar{p}}$. Note also that in case of perfect tracking of the reference position (which entails $\bar{p} = 0$, $\dot{\bar{p}} = 0$ and $\phi_c = 0$), it follows that, necessarily, $R'_c = I_3$ and $R_c = R_R$. Finally, the control inputs u_{f_1} and u_{f_2} are chosen as

$$\begin{aligned} u_{f_1} &= u^c_{f_1}(\bar{p}, \dot{\bar{p}}, \ddot{p}_R) := -e_3^T R_c^T v^c \\ u_{f_2} &= u^c_{f_2}(\bar{p}, \dot{\bar{p}}, \ddot{p}_R) := e_1^T R_c^T v^c = e_1^T R_R^T v^c \,. \end{aligned} \tag{18}$$

B. Attitude Controller

The group of rotations can be parameterized by means of a unit quaternion $q \in S_3$ through the mapping $\mathcal{R} : S_3 \to SO(3)$ (known as Rodriguez formula) defined as $\mathcal{R}(q) = I + 2\eta S(\epsilon) + 2S(\epsilon)^2$. The mapping $\mathcal{R}$ is such that $\mathcal{R}(q) = \mathcal{R}(-q)$, that is, the two quaternions q and $-q$ parameterize the same rotation matrix. Let the control quaternion $q_c = [\eta_c, \epsilon_c^T]^T \in S_3$ be such that $\mathcal{R}(q_c) = R_c$. With the control quaternion q_c at hand, it is possible to define the following attitude error coordinates

$$\bar{q} = q_c^{-1} \otimes q, \; \bar{w} := w - \bar{w}_c \tag{19}$$

with $\bar{w}_c := \mathcal{R}(\bar{q})^T w_c$ and then rewrite the attitude error dynamics in (1) – which is the same for both (VT4) and (VT5) – as

$$\begin{aligned} \dot{\bar{q}} &= \tfrac{1}{2}\bar{q} \otimes \begin{bmatrix} 0 \\ \bar{w} \end{bmatrix} \\ J\dot{\bar{w}} &= \Sigma(\bar{w}, \bar{w}_c)\bar{w} + S(J\bar{w}_c)\bar{w}_c - J\mathcal{R}(\bar{q})^T \dot{w}_c + u_\tau \,, \end{aligned} \tag{20}$$

having defined $\Sigma(\bar{w}, \bar{w}_c) := S(J\bar{w}) + S(J\bar{w}_c) - (S(\bar{w}_c)J + JS(\bar{w}_c))$. Following [20], we consider the hybrid controller

$$u_\tau = u_\tau^{FF}(\bar{q}, w_c, \dot{w}_c) + u_\tau^{FB}(\bar{q}, \bar{w}, \bar{h}) \tag{21}$$

where

$$\begin{aligned} u_\tau^{FF}(\bar{q}, w_c, \dot{w}_c) &= J\mathcal{R}(\bar{q})^T \dot{w}_c - S(J\bar{w}_c)\bar{w}_c \\ u_\tau^{FB}(\bar{q}, \bar{w}, \bar{h}) &= -k_p \bar{h}\bar{\epsilon} - k_d \bar{w} \end{aligned} \tag{22}$$

In system (22), k_p, k_d are positive gains and $\bar{h} \in \{-1, 1\}$ is obtained through the following hybrid dynamics

$$\mathcal{H}_c \quad \begin{cases} \dot{\bar{h}} = 0 & \bar{h}\bar{\eta} \geq -\delta \\ \bar{h}^+ \in \overline{\text{sgn}}(\bar{\eta}) & \bar{h}\bar{\eta} \leq -\delta \end{cases} \tag{23}$$

where $\delta \in (0, 1)$ is a hysteresis threshold and

$$\overline{\text{sgn}} = \begin{cases} \text{sgn}(s) & |s| > 0 \\ \{-1, 1\} & s = 0 \,. \end{cases}$$

The main idea behind the above choice of the attitude controller (21)-(22) is to exploit the properties of the design in [20] to guarantee that the attitude of the vehicle converges asymptotically to $\mathcal{R}(q_c)$, globally with respect to the initial attitude configuration $(R(0), w(0)) \in SO(3) \times \mathbb{R}^3$.

By combining the position controller (18) and the attitude controller (22), it is possible to prove the following result:

Proposition 1 *Consider system (3), where the control inputs are selected as in equations (18) and (22). Let the reference position and attitude trajectory $p_R(t)$, $R_R(t)$ be such that the constraints given in Section III-B are satisfied. For the attitude controller, let k_p and k_d be arbitrary positive numbers. For the position controller, let k_1, k_2, λ_1, λ_2 be selected as $\lambda_i = \epsilon^{(i-1)}\lambda_i^\star$, $k_i = \epsilon k_i^\star$, $i \in \{1, 2\}$ where $\epsilon > 0$ is a free parameter and $k_i^\star$, $\lambda_i^\star$ are fixed positive numbers that satisfy*

$$\frac{\lambda_2^\star}{k_2^\star} < \frac{\lambda_1^\star}{4}, \quad 4k_1^\star\lambda_1^\star < \frac{\lambda_2^\star}{4}, \quad 6\frac{k_1^\star}{k_2^\star} < \frac{1}{24} \tag{24}$$

Then there exists $\epsilon^\star > 0$ such that for all $0 < \epsilon < \epsilon^\star$

$$\lim_{t\to\infty} p(t) = p_R(t), \;\; \lim_{t\to\infty} R(t) = R_R(t) \tag{25}$$

for all initial conditions $(p(0), \dot{p}(0), R(0), w(0)) \in \mathbb{R}^3 \times \mathbb{R}^3 \times SO(3) \times \mathbb{R}^3$.

The above result shows how the proposed controller achieves global tracking of the desired time reference trajectory.

V. Experimental Results

The two-module ducted-fan prototype considered in this work has been specifically designed to accomplish operations requiring physical interaction with the surrounding environment. To achieve this goal, the system has been equipped with a docking mechanism and a compact robotic manipulator [21] suitable for aerial robotics applications. To take advantage of the dynamical model (3) characterizing this specific configuration, both the docking mechanism and the manipulator have been installed along the body x-axis.

$M = 3.8\ Kg$	$J = \text{diag}[0.1,\ 0.18,\ 0.16]\ Kg\,m^2$
$k_1^\star = \lambda_1^\star = 1$	$k_2^\star = \lambda_2^\star = 150$
$\epsilon = 0.2$	$(k_p,\ k_d) = (10,\ 6)$

TABLE I

PARAMETERS OF THE MODULAR DUCTED-FAN PROTOTYPE AND THE CONTROL LAW.

This device allows the vehicle to counteract the reaction forces deriving from physical interaction and to control the manipulator as if it has been installed on a fixed basis. The longitudinal dynamics of the vehicle in (3) is in fact fully-actuated thanks to the presence of the additional control input u_{f_2}. This latter, deriving from aerodynamic forces produced by the control surfaces, is only allowed to take values that are rather small compared to the main thrust produced by each propeller. In particular, experiments on a load cell [22] have shown how at hover, when each module has to produce approximately $18\ N$ of thrust to maintain the vehicle at hover, the maximum magnitude of the force u_{f_2} is approximately $6\ N$. Saturations on the admissible values of the input u_{f_2} have been accounted for in Section III through the definition of the set Ω_{f_2}. These constraints affect the admissible reference trajectories that can be achieved for the specific configuration.

The parameters of the prototype and of the control law employed in the experiments are given in Table I. Free-flight and physical interaction experiments are then presented in the following two subsections.

A. Free-Flight Experiments

Considering the model inversion obtained for both the (VT4) and (VT5) dynamics proposed in Section III, it is noted that one of the main advantages deriving from the additional input is the reduced number of constraints on the attitude of the system required to stabilize a desired position trajectory.

The free-flight experiment presented in this work aims at showing how the pitch angle of the vehicle can be changed while maintaining a constant position. The attitude and the position of the vehicle for this experiment are shown in Figures 2 and 3, respectively. Note that the system is able to achieve a pitch angle of approximately $8\ deg$ without accelerating along the inertial x-axis. The force inputs during the maneuver are presented in Figure 4.

B. Physical Interaction Experiments

In the last experiment proposed in this paper, the two-module vehicle is required to dock on a vertical surface. The surface is located at $x = 0.2\ m$ in the inertial frame. From the analysis of Figure 5, which shows the vehicle position in the inertial frame, it can be noted that the vehicle initially follows a trajectory approaching the surface with constant velocity. When the contact with the surface is established, the system applies a force of approximately $2\ N$ by means of the control input u_{f_2}, as shown in Figure 6. Finally, Figure 7 shows

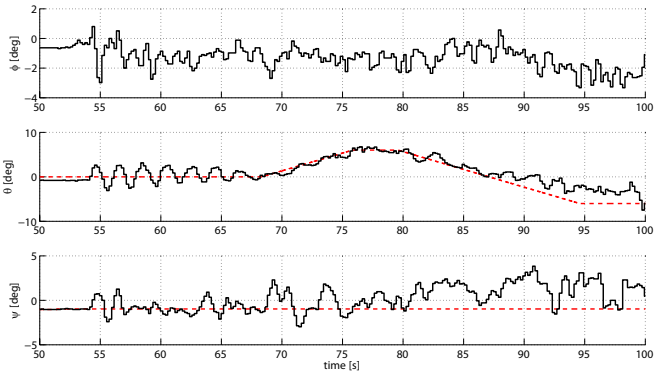

Fig. 2. The attitude of the prototype during the second experiment in which the vehicle is changing its attitude maintaining a constant position.

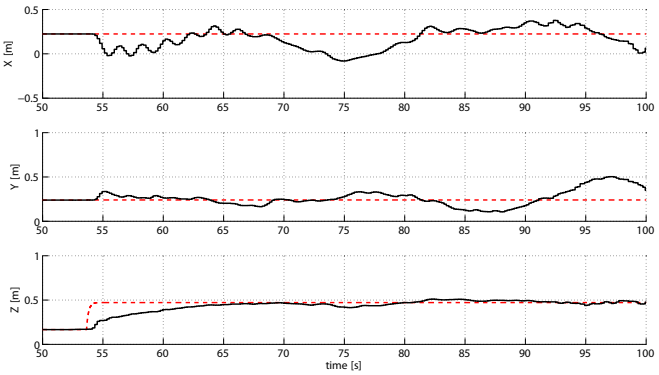

Fig. 3. The position of the prototype during the second experiment.

how this result is achieved without the vehicle changing significantly its attitude.

VI. CONCLUSION

This paper has presented a control strategy for global trajectory tracking for a class of vertical take-off and landing aerial systems characterized by redundancy in term of available control inputs. The proposed design allows to take advantage of the dynamic properties of the system by reducing the constraints on the achievable system trajectories, which is advantageous when performing tasks that require a high degree of dexterity, such as interaction with the environment. The control law has been validated experimentally by means of a prototype of modular aerial robot obtained by rigidly connecting two ducted-fan aerial vehicles. Future work will be focused on improving robustness of the closed-loop system, in particular with respect to aerodynamic disturbances.

REFERENCES

[1] E. Feron and E.N. Johnson. Aerial robotics. In B. Siciliano and O. Khatib, editors, *Springer Handbook of Robotics*, pages 1009–1027. Springer, 2008.

[2] V. Gavrilets, E. Frazzoli, B. Mettler, M. Piedimonte, and E. Feron. Aggressive maneuvering of small autonomous helicopters: A human-centered approach. *The International Journal of Robotics*, 20(10):795–807, 2001.

[3] E. Frazzoli, M. Dahleh, and E. Feron. Trajectory tracking control design for autonomous helicopters using a backstepping algorithm. *Proceedings of the American Control Conference*, pages 4102–4107, 2000.

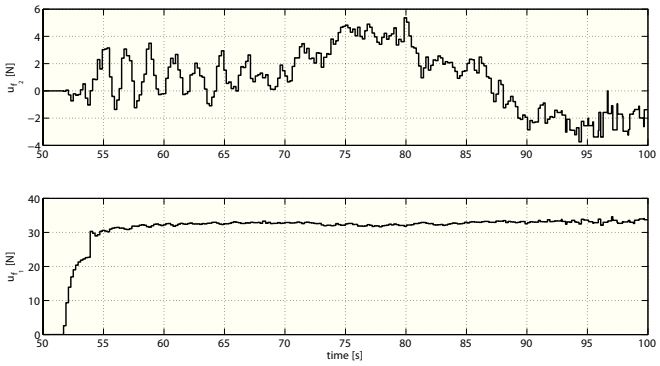

Fig. 4. The control forces u_{f_1} and u_{f_2} during the second experiment.

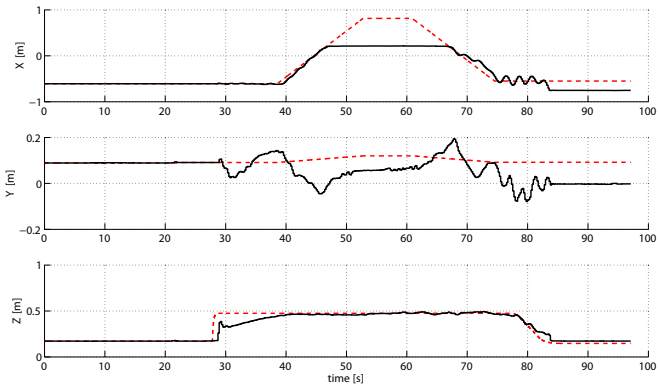

Fig. 5. The position of the prototype during the third experiment.

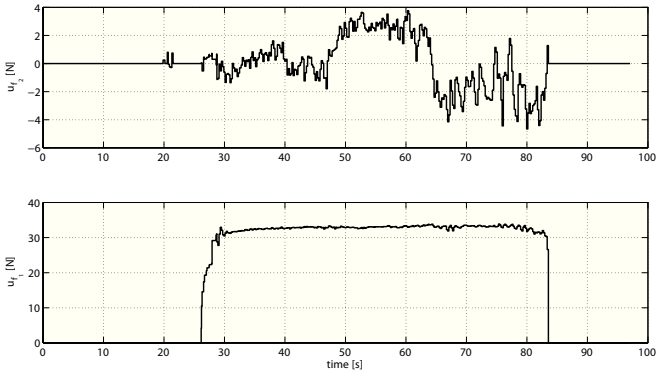

Fig. 6. The control forces u_{f_1} and u_{f_2} during the third experiment.

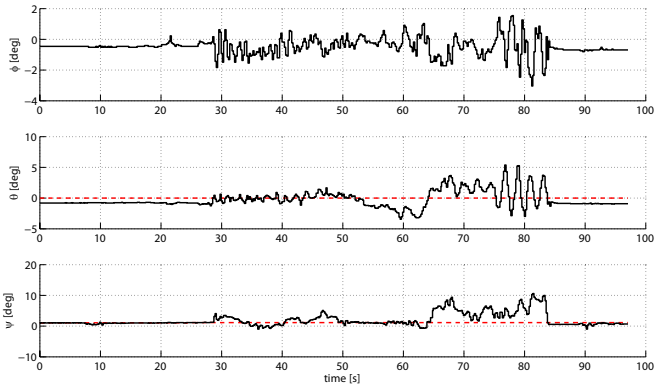

Fig. 7. The attitude of the prototype during the third experiment in which the vehicle is applying a force towards a surface without rotating.

[4] J.M. Pflimlin, P. Soueres, and T. Hamel. Hovering flight stabilization in wind gusts for ducted fan UAV. *42nd IEEE Conf. on Decision and Control*, 2004.

[5] R. Naldi, L. Gentili, L. Marconi, and A. Sala. Design and experimental validation of a nonlinear control law for a ducted-fan miniature aerial vehicle. *Control Engineering Practice*, 18(7):747–760, 2010.

[6] P. Pounds, R. Mahony, and P. Corke. Modelling and control of a large quadrotor robot. *Control Eng. Pract.*, 18(7):691–699, 2010.

[7] S. Bouabdallah and R. Siegwart. *Advances in Unmanned Aerial Vehicles*, chapter Chapter 6: Design and Control of a Miniature Quadrotor, pages 171–210. Springer Press, Feb. 2007.

[8] R. Cunha, D. Cabecinhas, and C. Silvestre. Nonlinear trajectory tracking control of a quadrotor vehicle. In *Proc. European Control Conference*, 2009.

[9] D. Mellinger, M. Shomin, N. Michael, and V. Kumar. Cooperative grasping and transport using multiple quadrotors. In *Proceedings of the International Symposium on Distributed Autonomous Systems*, Lausanne, Switzerland, 2010.

[10] M. Hua, T. Hamel, P. Morin, and C. Samson. Introduction to feedback control of underactuated VTOL vehicles. *IEEE Control Systems Magazine*, 33(2):61–75, February 2013.

[11] Christopher Korpela, Todd Danko, and Paul Oh. MM-UAV: Mobile manipulating unmanned aerial vehicle. *Journal of Intelligent & Robotic Systems*, pages 1–9, 2011.

[12] P. Pounds, D. Bersak, and A. Dollar. Grasping from the air: Hovering capture and load stability. In *Proceedings of the IEEE International Conference on Robotics and Automation*, 2011.

[13] F. Forte, R. Naldi, A. Macchelli, and L. Marconi. Impedance control of an aerial manipulator. In *Proceedings of the 2012 American Control Conference*, Montreal, CA, 2012.

[14] A. Albers, S. Trautmann, T. Howard, T.A. Nguyen, M. Frietsch, and C. Sauter. Semi-autonomous flying robot for physical interaction with environment. In *Proceedings of the IEEE Conference on Robotics Automation and Mechatronics (RAM)*, pages 441–446, Singapore, 2010.

[15] M. Ryll, H.H. Blthoff, and P.R. Giordano. Modeling and control of a quadrotor UAV with tilting propellers. In *Proceedings of 2012 IEEE International Conference on Robotics and Automation*, Saint Paul, Minnesota, US, 2012.

[16] R. Naldi, F.Forte, and L. Marconi. A class of modular aerial robots. In *Proceedings of the 50th IEEE Conference on Decision and Control*, Orlando, USA, 2011.

[17] F. Forte, R. Naldi, A. Serrani, and Marconi. Control of modular aerial robots. In *Proceedings of the 51st IEEE Conference on Decision and Control*, Maui, HI, 2012.

[18] M.D. Hua, T. Hamel, P. Morin, and C. Samson. A control approach for thrust-propelled underactuated vehicles and its applications to VTOL drones. *IEEE Transactions on Automatic Control*, 54(8):1837–1853, 2009.

[19] A. Isidori, L. Marconi, and A. Serrani. *Robust Autonomous Guidance: An Internal Model Approach*. Advances in Industrial Control. Springer-Verlag London, 2003.

[20] C.G. Mayhew, R.G. Sanfelice, and A.R. Teel. Quaternion-based hybrid controller for robust global attitude tracking. *IEEE Transactions on Automatic Control*, 56(11):2555–2566, November 2011.

[21] A.Q.L. Keemink, M. Fumagalli, S. Stramigioli, and R. Carloni. Mechanical design of a manipulation system for unmanned aerial vehicles. In *Proceedings of 2012 IEEE International Conference on Robotics and Automation*, pages 3147–3152, St. Paul, MN, 2012.

[22] R. Naldi and L. Marconi. Control allocation for a ducted-fan aerial robot employing both lift and drag forces. In *Proceedings of the 2012 American Control Conference*, Montreal, CA, 2012.

[23] J.L. Farrell. Attitude determination by Kalman filtering. *Automatica*, 6(3):419–430, 1970.

[24] H. K. Khalil. *Nonlinear systems*. Prentice Hall, 1996.